

## Supplementary Information

### Efficient CH<sub>4</sub> Oxidation to C1/C2 Oxygenates over Cluster-dispersing Rh decorated ZSM-5

Xin Zhang<sup>a</sup>, Wenzhi Li<sup>a,b\*</sup>, Jingting Jin<sup>a</sup>, Liquan Wang<sup>a</sup>, Zhiheng Lu<sup>c</sup>, Yihang Jiang<sup>a</sup>.

<sup>a</sup> Laboratory of Clean Low-Carbon Energy, Department of Thermal Science and Energy Engineering, University of Science and Technology of China, Hefei 230023, PR China.

<sup>b</sup> Institute of Energy, Hefei Comprehensive National Science Center, Hefei 230031, PR China.

<sup>c</sup> School of Earth and Environment, Anhui University of Science and Technology, Huainan 232001, PR China.

## Contents

<b>Contents .....</b>	<b>2</b>
<b>Supplementary Note 1 .....</b>	<b>5</b>
<i>Materials .....</i>	<i>5</i>
<i>Catalyst characterization and testing .....</i>	<i>5</i>
<b>Supplementary Note 2 .....</b>	<b>6</b>
<i>H<sub>2</sub> temperature-programmed reduction test (H<sub>2</sub>-TPR).....</i>	<i>6</i>
<i>CH<sub>4</sub>/ NH<sub>3</sub>/ CO<sub>2</sub> temperature-programmed desorption test (CH<sub>4</sub>/ NH<sub>3</sub>/ CO<sub>2</sub>-TPD)</i> <i>.....</i>	<i>7</i>
<i>In situ diffuse reflectance infrared Fourier transform spectroscopy (DRIFTS)</i> <i>measurements.....</i>	<i>7</i>
<i>High-performance liquid chromatography (HPLC).....</i>	<i>8</i>
<b>Fig. S1. (A) TEM images of 0.1 Rh/ZSM-5-IM, (B) 0.1 Rh/ZSM-5-AE .....</b>	<b>9</b>
<b>Fig. S2. (A) TEM images of 0.2 Rh/ZSM-5-IM, (B) 0.2 Rh/ZSM-5-AE, (C)</b> <b>0.4Rh/ZSM-5-IM, (D) 0.4 Rh/ZSM-5-AE, (E) 0.5 Rh/ZSM-5-IM and (F) 0.5</b> <b>Rh/ZSM-5-AE.....</b>	<b>10</b>
<b>Fig. S3. (A) Low-angle XRD results of ZSM-5, 0.3 Rh/ZSM-5-IM and 0.3 Rh/ZSM-</b> <b>5-AE. The detailed comparison results between the sample and (B) ZSM-5 (PDF#42-</b> <b>0305); (C) Rh (PDF#05-0685); (D) Rh<sub>2</sub>O<sub>3</sub> (PDF#71-2084).....</b>	<b>11</b>

<b>Fig. S4.</b> CO <sub>2</sub> -TPD curves of 0.3 Rh/ZSM-5-IM and 0.3 Rh/ZSM-5-AE.....	<b>12</b>
<b>Fig. S5.</b> DRIFT spectra of 0.3Rh/ZSM-5-IM (A) and 0.3Rh/ZSM-5-AE (B) obtained during dehydration at 30 °C-300 °C. ....	<b>13</b>
<b>Fig. S6.</b> Al 2p XPS spectra of 0.3 Rh/ZSM-5-IM and 0.3 Rh/ZSM-5-AE. ....	<b>14</b>
<b>Fig. S7.</b> Rh 3d XPS spectra of 0.3 Rh/ZSM-5-IM and 0.3 Rh/ZSM-5-AE. Rh <sup>0</sup> (cyan), Rh <sup>3+</sup> (red), Rh <sup>4+</sup> (brown).....	<b>15</b>
<b>Fig. S8.</b> NH <sub>3</sub> -TPD curves of 0.3 Rh/ZSM-5-IM and 0.3 Rh/ZSM-5-AE.....	<b>16</b>
<b>Fig. S9.</b> Effect of (A) different temperature for IM samples, (B) different temperature for AE samples.....	<b>17</b>
<b>Fig. S10.</b> Stability test of 0.3 Rh/ZSM-5-AE. ....	<b>18</b>
<b>Fig. S11.</b> (A) <sup>1</sup> H NMR spectra of liquid products using 0.3Rh/ZSM-5 catalyst; (B) GC-TCD signal for H <sub>2</sub> , O <sub>2</sub> , CO, CO <sub>2</sub> and CH <sub>4</sub> ; (C) HPLC signal for HCOOH and CH <sub>3</sub> COOH; (D) GC-FID signal for CH <sub>3</sub> OH and CH <sub>4</sub> .....	<b>19</b>
<b>Table S1.</b> ICP-AES data for 0.3Rh/ZSM-5-AE and 0.3Rh/ZSM-5-IM.....	<b>20</b>
<b>Table S2.</b> ICP-AES data for the supernatant.....	<b>21</b>
<b>Table S3.</b> Surface Chemical Composition of 0.3Rh/ZSM-5-AE and 0.3Rh/ZSM-5-IM .....	<b>22</b>
<b>Table S4.</b> Catalytic performance of 0.3Rh/ZSM-5-AE catalysts for the partial oxidation of methane under specific conditions .....	<b>23</b>

<b>Table S5.</b> Catalytic performance of different Rh loading for the partial oxidation of methane .....	<b>24</b>
-----------------------------------------------------------------------------------------------------------	-----------

<b>Table S6.</b> Catalytic performance of different temperature for the partial oxidation of methane .....	<b>25</b>
------------------------------------------------------------------------------------------------------------	-----------

<b>Table S7.</b> Catalytic performance of different temperature for the partial oxidation of methane .....	<b>26</b>
------------------------------------------------------------------------------------------------------------	-----------



## Supplementary Note 1

### *Materials*

ZSM-5 zeolites (Si/Al =25) were purchased from Nankai University Catalyst Co. Ammonia ( $\text{NH}_3 \cdot \text{H}_2\text{O}$ , 25%-28%) was purchased from Sinopharm Group Chemical Reagent Co. Rhodium nitrate dihydrate ( $\text{Rh}(\text{NO}_3)_3 \cdot 2(\text{H}_2\text{O})$ , 95%) was purchased from Shanghai Aladdin Biochemical Technology Co. All materials were not further purified.

### *Catalyst characterization and testing*

Inductively coupled plasma optical emission spectrometer (ICP-OES) was used to determine the Rh content in the synthesized catalysts. X-ray photoelectron spectroscopy (XPS), X-ray diffractometer patterns (XRD), spherical aberration-corrected transmission electron microscopy (AC-HAADF-TEM), transmission electron microscopy (TEM), in situ diffuse reflectance infrared Fourier transform spectroscopy (DRIFTS),  $\text{CH}_4/\text{NH}_3/\text{CO}_2$  temperature-programmed desorption test ( $\text{CH}_4$ -TPD) and  $\text{H}_2$  temperature-programmed reduction test ( $\text{H}_2$ -TPR) were used to characterize the physicochemical properties of the representative samples.

The catalytic performance of the synthesized catalysts was evaluated in a 100 mL 316L stainless steel batch reactor. Typically, 20 mg of catalyst was suspended in 20 mL of  $\text{H}_2\text{O}$ . The reactor was then sealed and purged three times with high-purity  $\text{O}_2$  to remove the air. The reactor was charged with 3 bar of high purity  $\text{O}_2$ , 8 bar of high purity CO and 20 bar of high purity  $\text{CH}_4$ , and the mixture was heated to the target temperature and kept under vigorous stirring for 30 min. At the end of the reaction, the

reactor was cooled in an ice bath after natural cooling to below 90 °C to minimize the loss of volatile products. After cooling, the liquid filtered from the catalyst particles was transferred to a 1.5 mL injection vial using a syringe with a filter and analyzed for methanol (The spectrum peak of CH<sub>3</sub>OH was at ~0.9min.) by an Agilent GC 7820A equipped with a Hydrogen Flame Ionisation Detector (FID) (using an HP-PLOT/Q column) and a Waters High Performance Liquid Chromatograph (HPLC) equipped with a Sugar-H column for formic and acetic acids. The gas products (The spectrum peaks of H<sub>2</sub>, O<sub>2</sub>, CO, CH<sub>4</sub> and CO<sub>2</sub> were at ~0.4, ~1, ~1.5, ~3.6 and ~10 min) were collected in a gas bag and analyzed by a gas chromatograph equipped with a thermal conductivity detector (TCD). Nuclear magnetic resonance hydrogen spectroscopy (1H NMR) were tested by adding 700 µL collected liquid into the 300 µL D<sub>2</sub>O (deuterated water). The 1H spectrum peaks of CH<sub>3</sub>COOH, CH<sub>3</sub>OH and HCOOH were at ~2.08, ~3.34 and ~8.24 ppm. Oxygenated compound yields and selectivity of each liquid oxygenated product were calculated by the following equations. Oxygenated compound *yield* (µmol/g<sub>cat</sub>/h) = Oxygenated compound *Amount* / *Catalyst Amount* / *Reaction Time*..... [1],

$$\text{Methyl Oxygenates Selectivity (\%)} = n[\text{CH}_3\text{OH} + \text{HCOOH} + \text{CH}_3\text{COOH}] / (n[\text{CO}_2] + n[\text{all liquid products}]) \times 100 \% \dots\dots [2].$$

## Supplementary Note 2

### *H<sub>2</sub> temperature-programmed reduction test (H<sub>2</sub>-TPR)*

H<sub>2</sub>-TPR was tested on a Japanese Microtrac BELCat II instrument equipped with a TCD detector. Typically, 100 mg of catalyst was transferred into a U-shaped quartz tube, warmed up from room temperature to 200 °C at a programmed rate of 10 °C/min for dry preconditioning, purged by He airflow (50 mL/min) for 1 h, cooled down to 50 °C, and passed into a 10% H<sub>2</sub>/Ar mixture (50 mL/min) for 0.5 h. After the base line was stable, the samples were detached at 800 °C in a 10% H<sub>2</sub>/Ar gas stream at a heating rate of 10 °C/min. The reducing gas was detected by TCD, and the H<sub>2</sub>-TPR curves were recorded from 50 to 700 °C.

***CH<sub>4</sub>/NH<sub>3</sub>/CO<sub>2</sub> temperature-programmed desorption test (CH<sub>4</sub>/NH<sub>3</sub>/CO<sub>2</sub>-TPD)***

The CH<sub>4</sub>/NH<sub>3</sub>/CO<sub>2</sub>-TPD test was conducted using the same instrument and followed a procedure similar to that of the H<sub>2</sub>-TPR test, with a few modifications. Initially, the inlet gas was switched to a methane atmosphere for 1 hour to achieve saturation. Subsequently, the gas was switched to He at a flow rate of 50 mL/min for 1 hour to remove weakly physically absorbed CH<sub>4</sub>/NH<sub>3</sub>/CO<sub>2</sub> from the surface. Following this, the sample was desorbed at 800 °C under a He atmosphere, with the temperature increased at a rate of 10 °C/min. The desorbed gases were then detected using a TCD, and the CH<sub>4</sub>/NH<sub>3</sub>/CO<sub>2</sub>-TPD curves were recorded over a temperature range of 50 to 700 °C

***In situ diffuse reflectance infrared Fourier transform spectroscopy (DRIFTS) measurements***

In situ DRIFTS measurements were carried out using a Niolet iS50 FTIR

spectrometer equipped with a DTGS KBr detector to assess possible reaction mechanisms on the catalyst surface and to characterize the structure of metal Rh species. Spectral results were recorded for 32 scans at a resolution of  $4\text{ cm}^{-1}$  by means of a mercury cadmium telluride (MCT) detector and a high-temperature reaction chamber with a recirculating  $\text{H}_2\text{O}$  cooling system. The chamber was purged with Ar (2 mL/min) for 30 min at room temperature to minimize the effect of residual gas in the line. The gas line valve was then closed, the sample was loaded into the reaction chamber, and the background spectra were collected after warming up to  $240\text{ }^\circ\text{C}$ . At  $240\text{ }^\circ\text{C}$ , the distributions were recorded with inputs of a mixed atmosphere of  $\text{CH}_4$  and  $\text{O}_2$  ( $\text{CH}_4:\text{O}_2 = 20:3$ ) and a mixed atmosphere of  $\text{CH}_4$ ,  $\text{O}_2$  and  $\text{CO}$  ( $\text{CH}_4:\text{O}_2:\text{CO} = 20:8:3$ ). In probing the surface states of Rh species, the steps were similar, with the exception that the input gas was replaced with  $\text{CO}$ , and each set of data was collected after 30 min of  $\text{CO}$  passages followed by 30 min of Ar gas purging.

#### ***High-performance liquid chromatography (HPLC)***

The quantitative analysis of formic acid and acetic acid (The spectrum peaks of  $\text{HOCCH}$  and  $\text{CH}_3\text{COOH}$  were at  $\sim 13.44$  and  $\sim 14.5$  min) were determined by high-performance liquid chromatography (HPLC, Waters 515 pump), which has a Sugar-H column ( $8\mu\text{m}$ ,  $7.8 \times 300\text{mm}$ ) and a differential refractive index detector (Waters 2414), using a 0.1 vol.%  $\text{C}_2\text{HF}_3\text{O}_2$  solution as the mobile phase. The column and detector temperature was set at  $60$  and  $50\text{ }^\circ\text{C}$ , respectively, and the flow rate was controlled at  $0.6\text{ mL/min}$ .

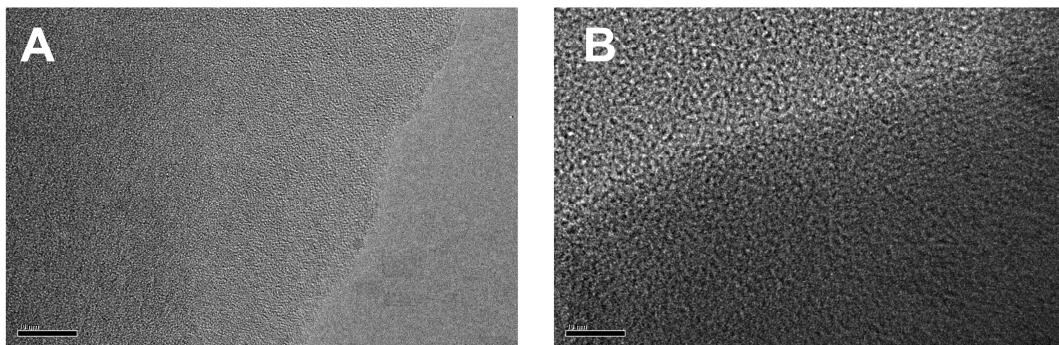


**Fig. S1. (A)** TEM images of 0.1 Rh/ZSM-5-IM, **(B)** 0.1 Rh/ZSM-5-AE (The scale bar in TEM images is 10 nm)

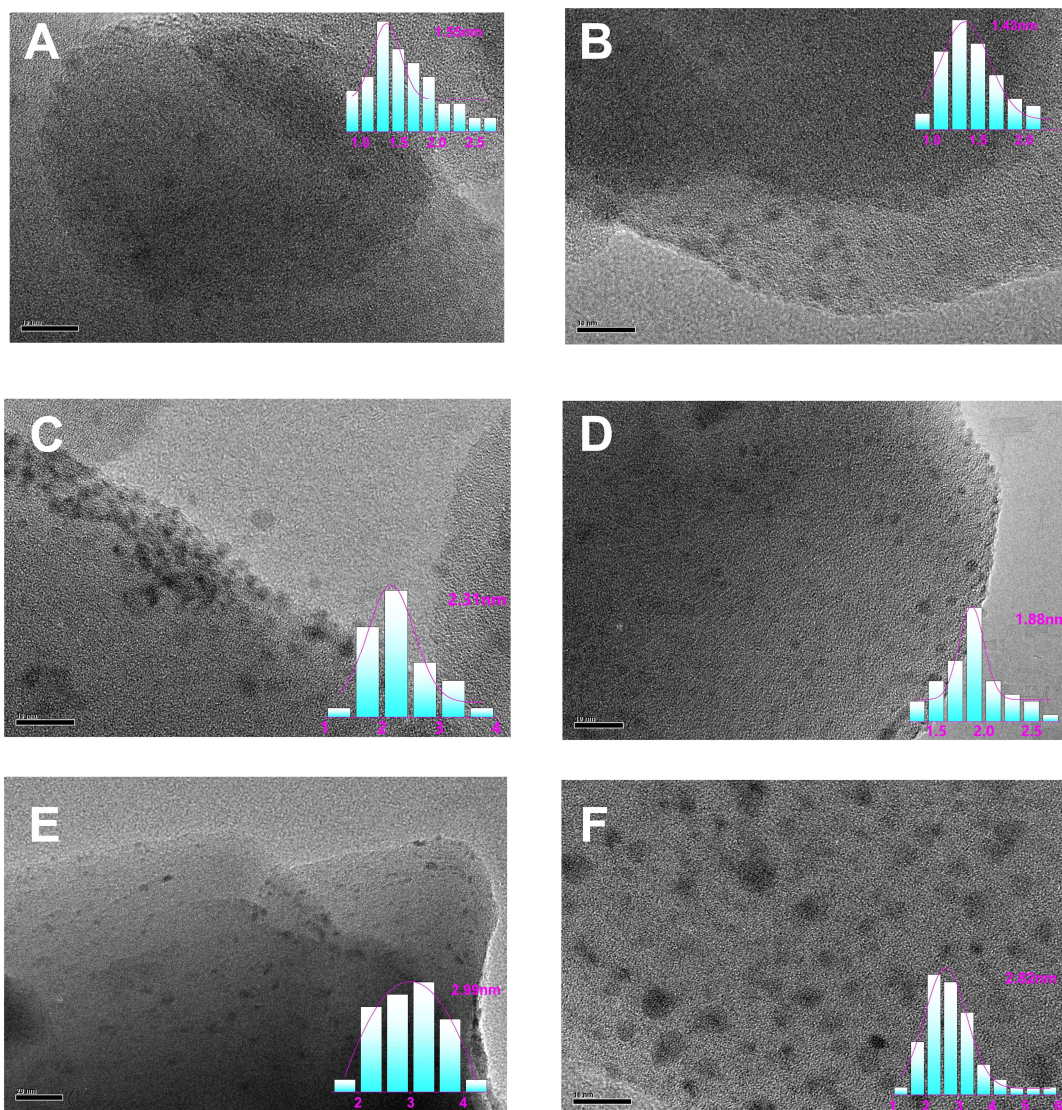


**Fig. S2.** (A) TEM images of 0.2 Rh/ZSM-5-IM, (B) 0.2 Rh/ZSM-5-AE, (C) 0.4Rh/ZSM-5-IM, (D) 0.4 Rh/ZSM-5-AE, (E) 0.5 Rh/ZSM-5-IM and (F) 0.5 Rh/ZSM-5-AE (The scale bar in TEM images is 10 nm)

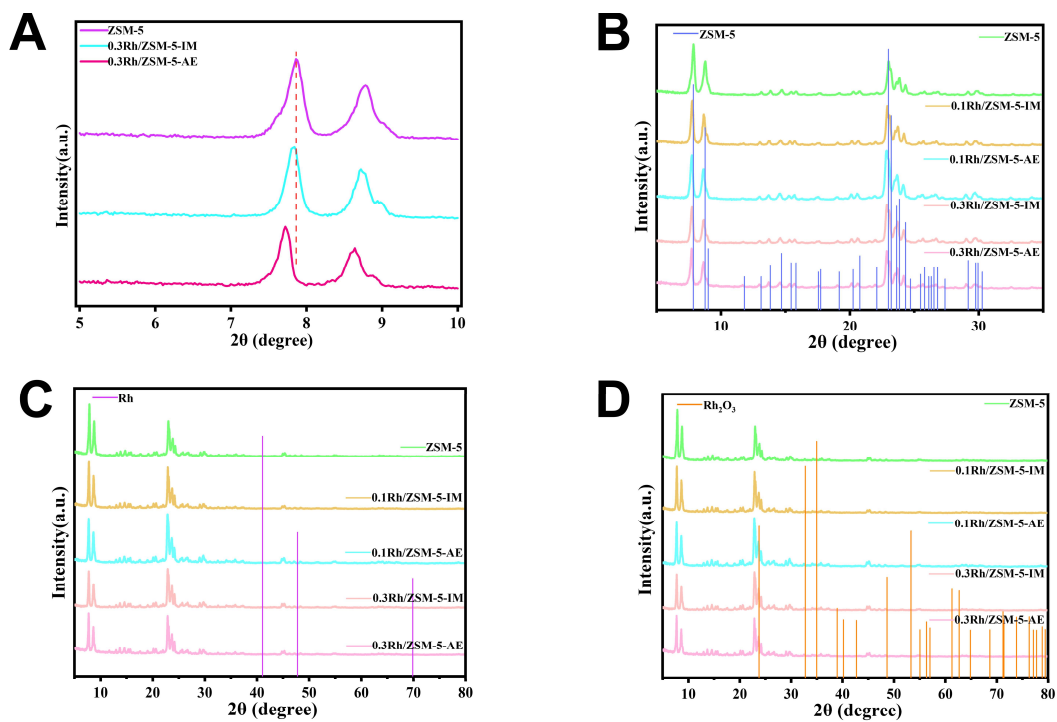


**Fig. S3.** (A) Low-angle XRD results of ZSM-5, 0.3 Rh/ZSM-5-IM and 0.3 Rh/ZSM-5-AE. The detailed comparison results between the sample and (B) ZSM-5 (PDF#42-0305); (C) Rh (PDF#05-0685); (D) Rh<sub>2</sub>O<sub>3</sub> (PDF#71-2084).

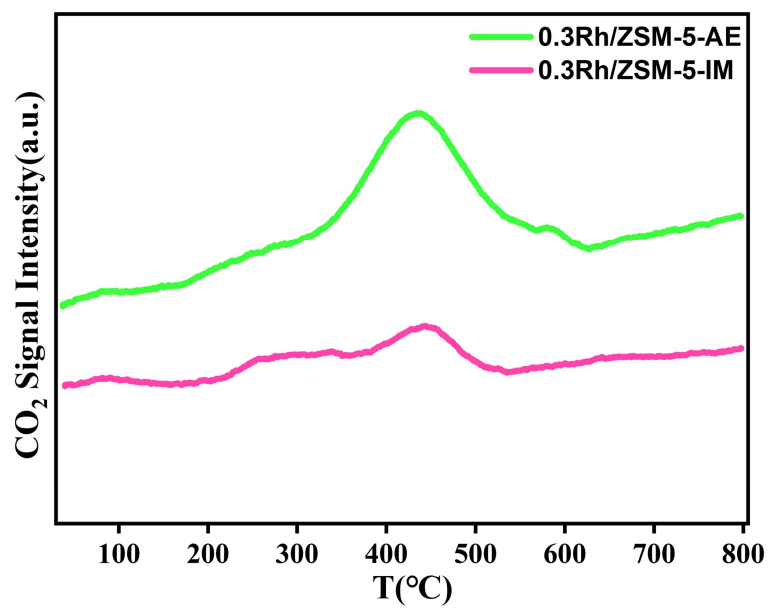


**Fig. S4.** CO<sub>2</sub>-TPD curves of 0.3 Rh/ZSM-5-IM and 0.3 Rh/ZSM-5-AE.



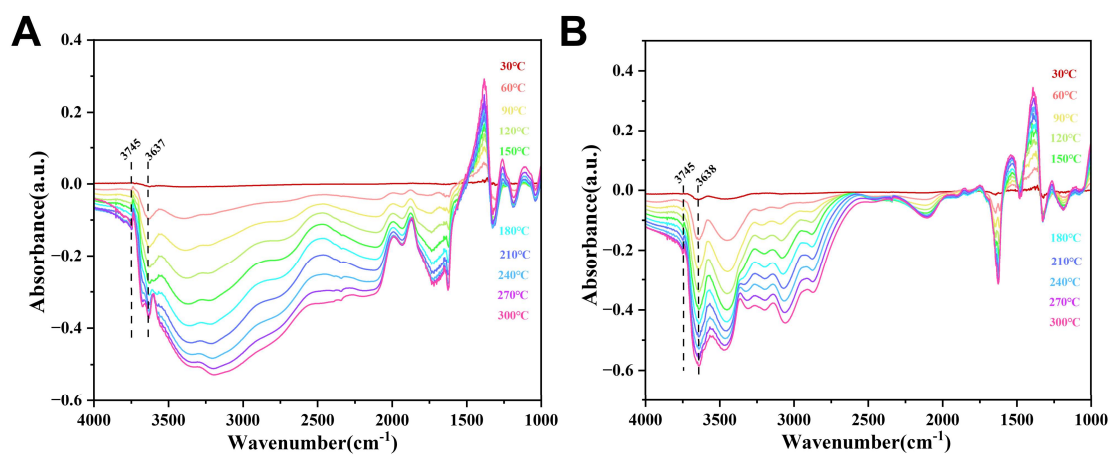


**Fig. S5.** DRIFT spectra of 0.3Rh/ZSM-5-IM (**A**) and 0.3Rh/ZSM-5-AE (**B**) obtained during dehydration at 30 °C-300 °C.

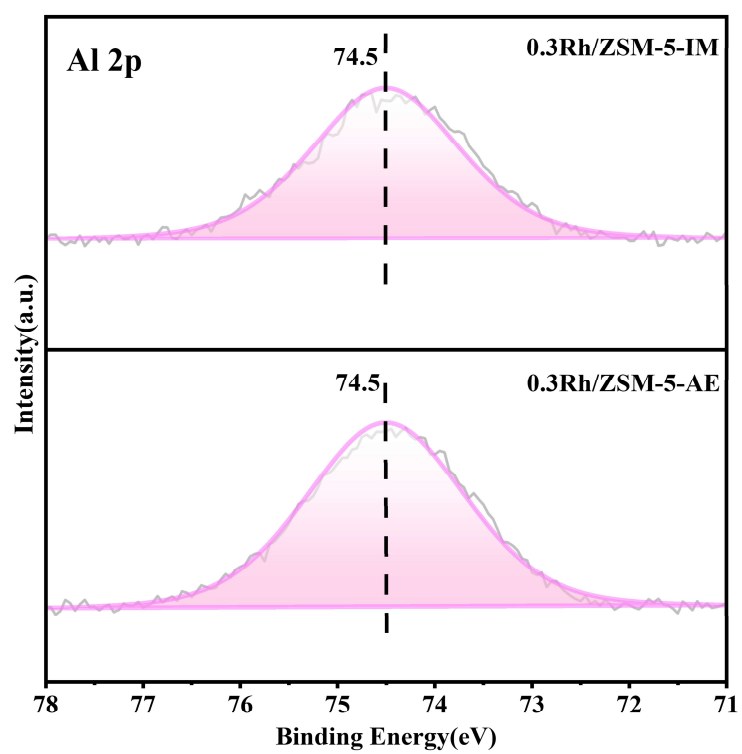


**Fig. S6.** Al 2p XPS spectra of 0.3 Rh/ZSM-5-IM and 0.3 Rh/ZSM-5-AE.

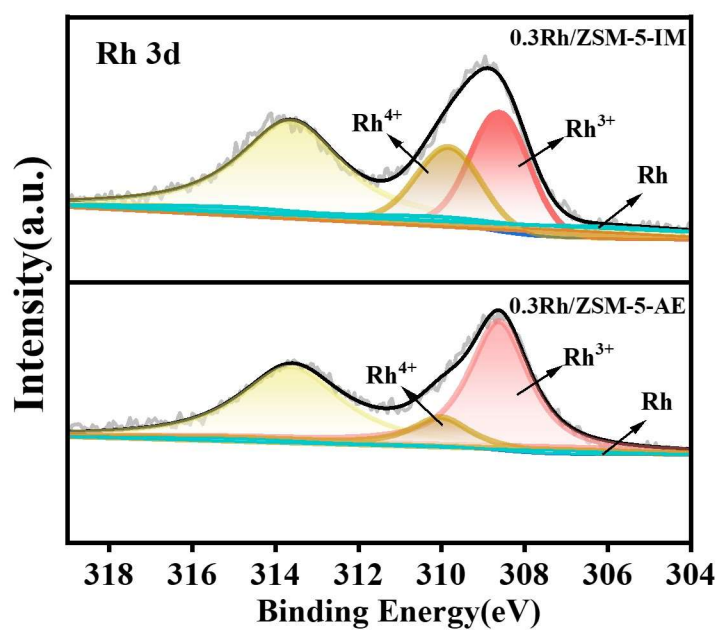


**Fig. S7.** Rh 3d XPS spectra of 0.3 Rh/ZSM-5-IM and 0.3 Rh/ZSM-5-AE. Rh<sup>0</sup>(cyan), Rh<sup>3+</sup>(red), Rh<sup>4+</sup>(brown).

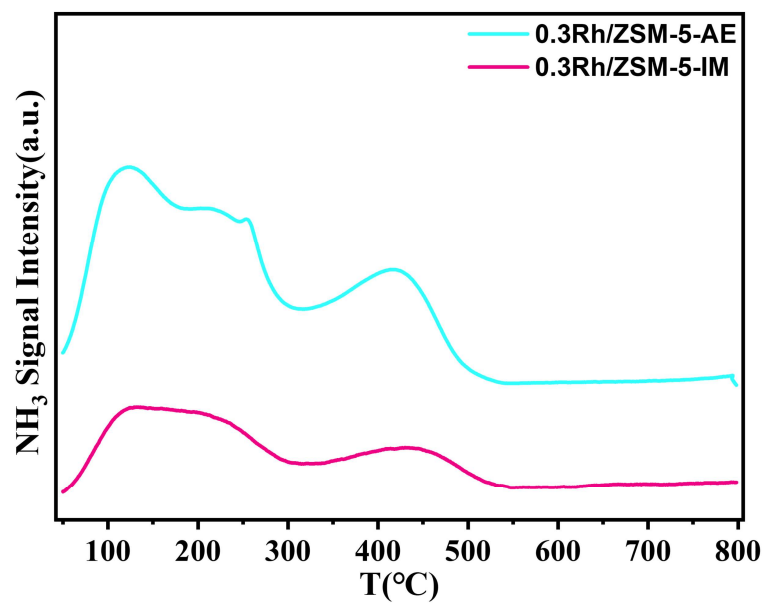


**Fig. S8.** NH<sub>3</sub>-TPD curves of 0.3 Rh/ZSM-5-IM and 0.3 Rh/ZSM-5-AE.

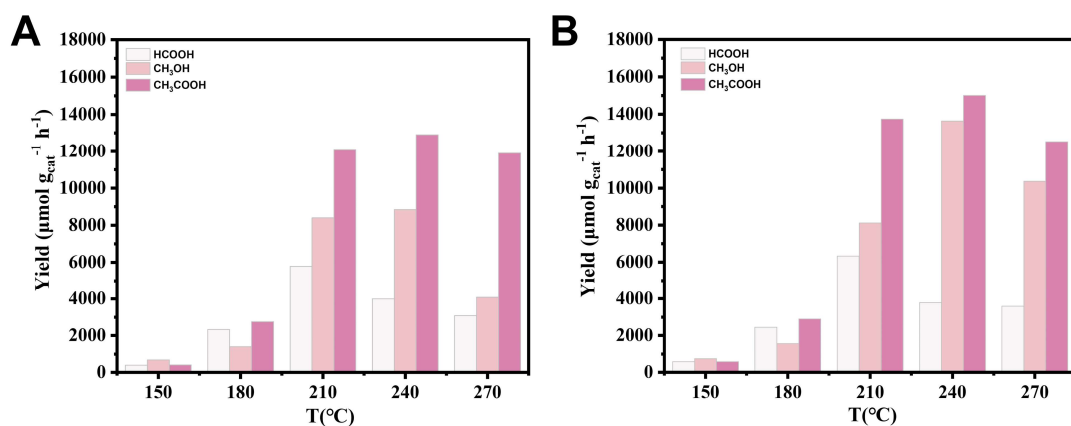


**Fig. S9.** Effect of **(A)** different temperature for IM samples, **(B)** different temperature for AE samples (Reaction conditions:  $P_{\text{CH}_4} = 20$  bar,  $P_{\text{CO}} = 8$  bar,  $P_{\text{O}_2} = 3$  bar, 20 mL water, 20 mg catalyst, 0.5 h at different temperature)

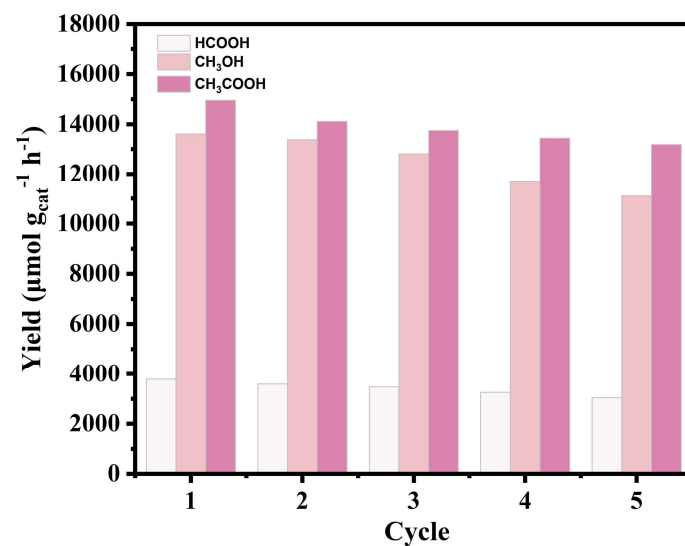


**Fig. S10.** Stability test of 0.3 Rh/ZSM-5-AE. (Reaction conditions:  $P_{\text{CH}_4} = 20$  bar,  $P_{\text{CO}} = 8$  bar,  $P_{\text{O}_2} = 3$  bar, 20 mL water, 20 mg catalyst, 0.5 h at 240°C)

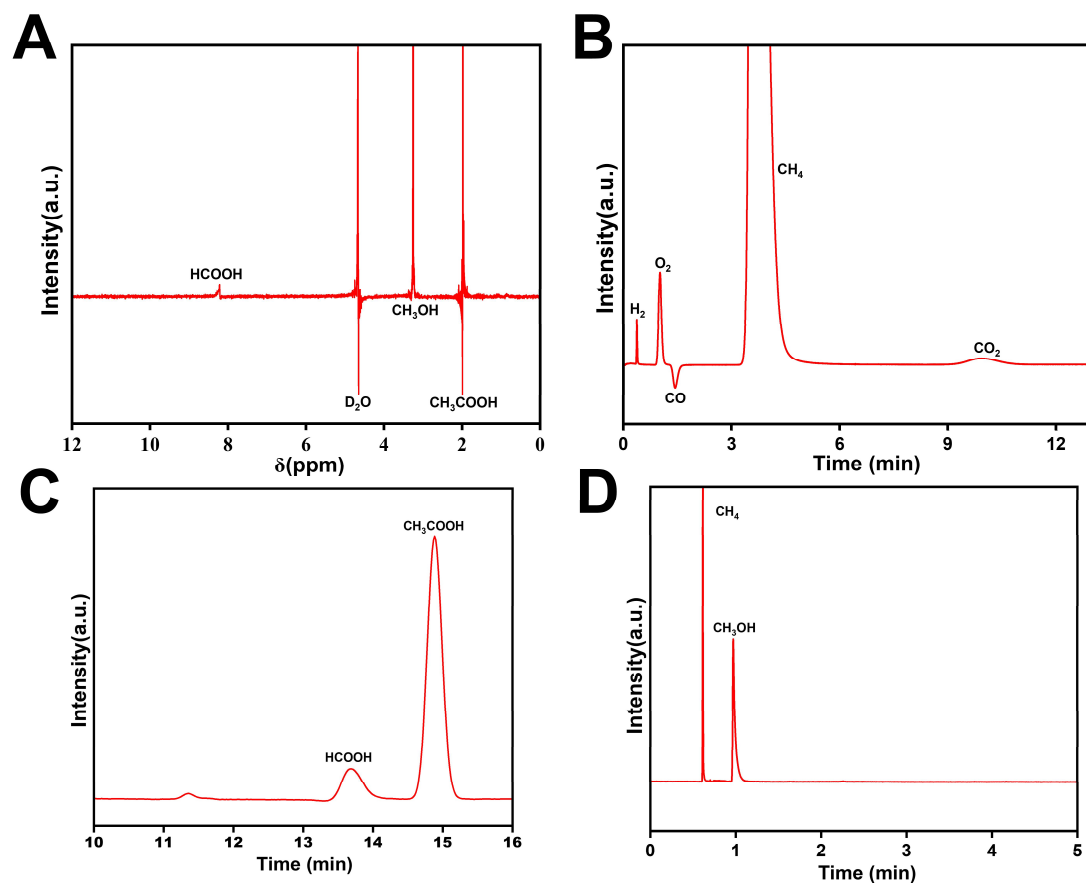


**Fig. S11.** (A)  $^1\text{H}$  NMR spectra of liquid products using 0.3Rh/ZSM-5-AE catalyst; (B) GC-TCD signal for  $\text{H}_2$ ,  $\text{O}_2$ , CO,  $\text{CO}_2$  and  $\text{CH}_4$ ; (C) HPLC signal for HCOOH and  $\text{CH}_3\text{COOH}$ ; (D) GC-FID signal for  $\text{CH}_3\text{OH}$  and  $\text{CH}_4$ .

**Table S1.** ICP-OES data for 0.3Rh/ZSM-5-AE and 0.3Rh/ZSM-5-IM

Entry	Catalyst	Test element	Sample element content W (%)
1	0.3Rh/ZSM-5-AE	Al	3.13
2	0.3Rh/ZSM-5-IM	Al	2.93
3	0.3Rh/ZSM-5-AE	Si	43.70
4	0.3Rh/ZSM-5-IM	Si	43.81
5	0.3Rh/ZSM-5-AE	Rh	0.35
6	0.3Rh/ZSM-5-IM	Rh	0.34



**Table S2.** ICP-OES data for the supernatant

Entry	Supernatant	Test element	Mass fraction (µg/mL)
1	supernatant -AE	Al	0.12
2	supernatant -IM	Al	0
3	supernatant -AE	Si	29.27
4	supernatant -IM	Si	0

Supernatant-AE is the supernatant collected by centrifugation during the preparation of the 0.3 Rh/ZSM-5-AE catalyst; supernatant-IM is the supernatant collected by centrifugation of 0.3Rh/ZSM-5-IM samples in deionized water at room temperature for one hour, followed by heating to 90 °C for another hour.

**Table S3. Surface Chemical Composition of 0.3Rh/ZSM-5-AE and 0.3Rh/ZSM-5-IM**

Entry	Samples	$\text{Rh}^0/$ ( $\text{Rh}^0 + \text{Rh}^{3+} +$ $\text{Rh}^{4+}$ ), %	$\text{Rh}^{3+}/$ ( $\text{Rh}^0 + \text{Rh}^{3+} +$ $\text{Rh}^{4+}$ ), %	$\text{Rh}^{4+}/$ ( $\text{Rh}^0 + \text{Rh}^{3+} +$ $\text{Rh}^{4+}$ ), %
1	0.3Rh/ZSM-5-IM	25.36	43.85	30.79
2	0.3Rh/ZSM-5-AE	<0.01	75.83	24.17

**Table S4.** Catalytic performance of 0.3Rh/ZSM-5-AE catalysts for the partial oxidation of methane under specific conditions

Entry	Reaction atmosphere (bar)	Productivity ( $\mu\text{mol}\cdot\text{g}_{\text{cat}}^{-1}\cdot\text{h}^{-1}$ )		
		CH <sub>3</sub> OH	HCOOH	CH <sub>3</sub> COOH
1	CH <sub>4</sub> (20) + O <sub>2</sub> (3) + N <sub>2</sub> (8)	<5	<5	<5
2	N <sub>2</sub> (20) + O <sub>2</sub> (3) + CO (8) + CH <sub>3</sub> OH	19638.12	<5	<5
3	CH <sub>4</sub> (20) + O <sub>2</sub> (3) + N <sub>2</sub> (8) + CH <sub>3</sub> OH	19568.45	<5	<5
4	N <sub>2</sub> (20) + O <sub>2</sub> (3) + CO (8) + HCOOH	<5	22483.56	<5
5	CH <sub>4</sub> (20) + O <sub>2</sub> (3) + N <sub>2</sub> (8) + HCOOH	<5	23225.39	<5

Reaction conditions: catalyst 0.3Rh/ZSM-5-AE (20 mg), water (20mL), temperature (240°C), CH<sub>3</sub>OH (10 $\mu$ L), HCOOH (10 $\mu$ L).

**Table S5.** Catalytic performance of different Rh loading for the partial oxidation of methane

Entry	Sample	Productivity ( $\mu\text{mol}\cdot\text{g}_{\text{cat}}^{-1}\cdot\text{h}^{-1}$ )		
		CH <sub>3</sub> OH	HCOOH	CH <sub>3</sub> COOH
1	0.1Rh/ZSM-IM	524.46	332.13	984.37
2	0.2 Rh/ZSM-IM	4740.76	1204.43	6530.28
3	0.3 Rh/ZSM-IM	8840.63	3993.25	12911.45
4	0.4 Rh/ZSM-IM	4210.38	2210.66	7640.73
5	0.5 Rh/ZSM-IM	3650.49	1780.58	7320.26
6	0.1 Rh/ZSM-AE	533.29	480.24	1560.46
7	0.2 Rh/ZSM-AE	8397.74	3750.85	10354.28
8	0.3 Rh/ZSM-AE	13640.53	3787.33	15005.47
9	0.4 Rh/ZSM-AE	7920.43	3560.36	11980.69
10	0.5 Rh/ZSM-AE	8200.62	2760.72	9700.54

Reaction conditions: P<sub>CH<sub>4</sub></sub> = 20 bar, P<sub>CO</sub> = 8 bar, P<sub>O<sub>2</sub></sub> = 3 bar, 20 mL water, 20 mg catalyst, 0.5 h at 240 °C

**Table S6.** Catalytic performance of different temperature for the partial oxidation of methane

Entry	Sample	Temperature (°C)	Productivity ( $\mu\text{mol}\cdot\text{g}_{\text{cat}}^{-1}\cdot\text{h}^{-1}$ )		
			CH <sub>3</sub> OH	HCOOH	CH <sub>3</sub> COOH
1	0.3 Rh/ZSM-IM	150	675.43	395.14	412.73
2	0.3 Rh/ZSM-IM	180	1400.37	2325.32	2756.94
3	0.3 Rh/ZSM-IM	210	8400.76	5783.34	12063.36
4	0.3 Rh/ZSM-IM	240	8840.63	3993.25	12911.45
5	0.3 Rh/ZSM-IM	270	4080.69	3082.29	11900.65
6	0.3 Rh/ZSM-AE	150	740.84	586.12	580.84
7	0.3 Rh/ZSM-AE	180	1560.64	2448.24	2899.65
8	0.3 Rh/ZSM-AE	210	8120.62	6335.22	13743.48
9	0.3 Rh/ZSM-AE	240	13640.53	3787.33	15005.47
10	0.3 Rh/ZSM-AE	270	10368.49	3587.76	12530.45

Reaction conditions:  $P_{\text{CH}_4} = 20$  bar,  $P_{\text{CO}} = 8$  bar,  $P_{\text{O}_2} = 3$  bar, 20 mL water, 20 mg catalyst, 0.5 h at different temperature.

**Table S7.** Catalytic performance of different temperature for the partial oxidation of methane

Entry	Reaction condition (bar)	Productivity ( $\mu\text{mol}\cdot\text{g}_{\text{cat}}^{-1}\cdot\text{h}^{-1}$ )		
		CH <sub>3</sub> OH	HCOOH	CH <sub>3</sub> COOH
1	CH <sub>4</sub> (0) + O <sub>2</sub> (3) + CO (5)	0	0	0
2	CH <sub>4</sub> (8) + O <sub>2</sub> (3) + CO (5)	756.35	132.65	563.25
3	CH <sub>4</sub> (12) + O <sub>2</sub> (3) + CO (5)	1832.56	325.65	4562.35
4	CH <sub>4</sub> (16) + O <sub>2</sub> (3) + CO (5)	7523.65	963.15	7952.26
5	CH <sub>4</sub> (20) + O <sub>2</sub> (3) + CO (5)	8935.64	1587.22	10032.73
6	CH <sub>4</sub> (24) + O <sub>2</sub> (3) + CO (5)	12980.89	2384.15	12707.28
7	CH <sub>4</sub> (15) + O <sub>2</sub> (3) + CO (0)	0	0	0
8	CH <sub>4</sub> (15) + O <sub>2</sub> (3) + CO (4)	1832.72	396.57	5324.26
9	CH <sub>4</sub> (15) + O <sub>2</sub> (3) + CO (6)	7785.36	945.56	8006.49
10	CH <sub>4</sub> (15) + O <sub>2</sub> (3) + CO (8)	8405.47	1382.25	8621.58
11	CH <sub>4</sub> (15) + O <sub>2</sub> (3) + CO (12)	8581.95	1610.76	8847.85
12	CH <sub>4</sub> (15) + O <sub>2</sub> (3) + CO (16)	8462.46	1853.16	8975.64

Reaction conditions: 20 mL water, 20 mg 0.3 Rh/ZSM-AE catalyst, 0.5 h at 240 °C